Journal of Power Sources 601 (2024) 234271

Contents lists available at ScienceDirect

Journal of Power Sources

journal homepage: www.elsevier.com/locate/jpowsour

High-pressure PEM water electrolyser performance up to 180 bar differential pressure

Ragnhild Hancke *, Piotr Bujlo, Thomas Holm, Øystein Ulleberg

Institute for Energy Technology, Department for Hydrogen Technology, Instituttveien 18, 2007, Kjeller, Norway

HIGHLIGHTS

- High-pressure prototype PEMEL stack was operated up to 180 bar pressure.
- Pressurized operation yields lower efficiency than expected from model.
- Safety issues related to hydrogen crossover are measured and discussed.

ABSTRACT

Proton exchange membrane (PEM) electrolysers (PEMEL) are key for converting and storing excess renewable energy. PEMEL water electrolysis offers benefits over alkaline water electrolysers, including a large dynamic range, high responsiveness, and high current densities and pressures. High operating pressures are important because it contributes to reduce the costs and energy-use related to downstream mechanical compression. In this work the performance of a high-pressure PEMEL system has been characterized up to 180 bar. The electrolyser stack has been characterized with respect to electrochemical performance, net H_2 production rate, and water crossover, and the operability and performance of the thermal- and gas management systems of the test bench has been assessed. The tests show that the voltage increase upon pressurization from 5 to 30 bar is 30 % smaller than expected, but further pressurization reduces performance. The study confirms that high-pressure PEMEL has higher energy consumption than state-of-the-art electrolyser systems with mechanical compressors. However, there can be a business case for high-pressure PEMEL if the trade-off between stack efficiency and system efficiency is balanced.

1. Introduction

One of the possibilities to reduce the costs of green hydrogen is to increase the operating pressure of the water electrolyser and thereby reduce the need for mechanical hydrogen compression. State-of-the-art commercial PEM water electrolyser systems operate at hydrogen outlet pressures of 30–40 bar, but there are many end-use applications which require considerably higher pressure-levels, e.g., injection into the natural gas grid (ca. 70 bar), green methanol production (ca. 80 bar), and ammonia production (ca. 200 bar). These, and other potential uses for green hydrogen, are listed in Fig. 1 together with their required pressure levels. Thus, by increasing the hydrogen outlet pressure of the electrolyser to any of these pressure levels, it will be possible to omit the mechanical compressor completely, and thereby remove a component which adds significant system complexity and costs.

In a previous work, we showed that electrochemical compression to all the assessed pressure levels (80–700 bar) requires more energy than utilizing state-of-the-art electrolysers delivering H_2 at 30 bar combined with a mechanical compressor [1]. The added energy cost can however be compensated by the achieved reduction in capital expenditure (CAPEX) through the removal of the compressor, and the business case for high-pressure PEMEL therefore depends on *i)* the electricity price and *ii)* the cost penalty of implementing high-pressure PEMEL systems. With an electricity price of 0.12 € kWh^{-1} (which was the EU average for industrial consumers in 2020), we have shown that 80 bar PEM water electrolysis system is more cost efficient than a 30 bar system combined with a mechanical compressor as long as the PEMEL system CAPEX does not increase more than 12% from the baseline electrolyser stack cost for commercial systems of 900 € kW^{-1}.

Although PEM electrolysers today deliver hydrogen at 30–40 bar, it is possible to achieve self-pressurizing systems compatible with all the end uses listed in Fig. 1 [2–4]. This is enabled by the solid polymeric membrane which supports very large pressure gradients across the cells, in contrast to alkaline systems which can only be operated with balanced pressure [5]. One of the advantages of differential pressure PEMELs, is that there is no need to handle compressed oxygen gas or to install

* Corresponding author.
E-mail address: Ragnhild.Hancke@ife.no (R. Hancke).

https://doi.org/10.1016/j.jpowsour.2024.234271
Received 15 November 2023; Received in revised form 9 February 2024; Accepted 26 February 2024
Available online 7 March 2024

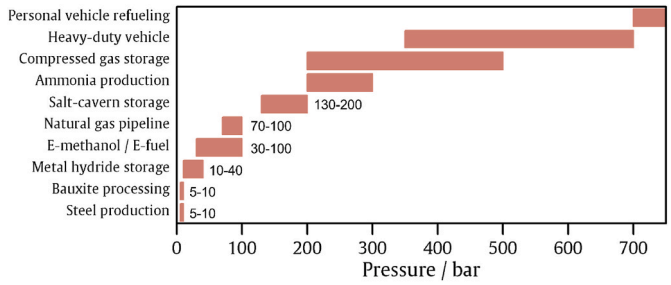

Fig. 1. Examples of possibles use cases for green hydrogen and the needed pressure levels. (For interpretation of the references to colour in this figure legend, the reader is referred to the Web version of this article.)

high-pressure components in the oxygen sub-systems, meaning that the associated safety challenge and added system capital costs are avoided [2,6,7]. Differential-pressure electrolysers furthermore produce higher purity hydrogen than thosed based on balanced pressure.

A main challenge of PEMELs operating under large pressure gradients is the associated high hydrogen diffusion rate through the membrane from the hydrogen to the oxygen side [7–14]. This phenomenon effectively decreases the current yield of the system. To avoid hydrogen concentration on the oxygen side exceeding the lower flammability limit (LFL) of 4 vol%, it is also necessary to incorporate anodic gas recombination catalysts [15] and exercise load-following operation with care. Differential pressure systems also have higher requirements for mechanical strength. This is particularly the case for the anode cell components which must withstand the pressure from the cathode side [12, 16]. The use of thick or reinforced membranes and porous transport layers may therefore be required, adding cost and resulting in higher ohmic losses.

To realize high-pressure electrolysis, more R&D is required to improve the stacks and systems by addressing safety, efficiency, durability, and CAPEX. It is also crucial to have validated high-pressure stack- and system models that can predict efficiency and durability while operating at elevated pressures in order to optimize design and operation of these systems. Only a few experimental studies characterizing PEMEL stack performance under high-pressure conditions have previously been carried out. These studies include testing of a 70 bar stack from Giner Labs (6 kW) at Politecnico di Torino [17–19], a 155 bar stack from Fronius (10 kW) at HyCentA Research GmbH in Graz [20], a 130 bar stack developed in the GenHyPEM project (1 Nm^3h^{-1}) [4], and a 57 bar stack from Proton-On-Site [21]. For single-cell experiments, the test bench development and electrochemical characterization of a 100 bar single cell developed at PSI [22], the 110 bar test bench at Esslingen University of Applied Sciences [23], and the 113 bar test bench at Tsinghua University [12] are good examples of ongoing research. In addition to these experimental campaigns, several theoretical studies have been carried out aiming to understand the loss processes and to achieve safe and efficient operation [1,11,19,24–27].

Although the topic of high-pressure electrolysis is receiving increased attention, the available experimental data is too fragmented and scattered to form a basis for optimized design and operation. A fundamental understanding of the effect of pressure on electrolyser performance is, furthermore, still lacking. In this paper we present system performance data obtained from operating a prototype stack as a function of current density between 5 and 180 bar H_2 outlet pressure at 30 °C, 50 °C and 80 °C. The efficiency losses associated with pressure- and temperature variations are assessed and compared with previous models. The tests show that high-pressure operation leads to higher efficiency-losses than previously modelled [1], but also shows that there can be a business case for high-pressure PEMEL if the trade-off between the stack efficiency and system efficiency can be balanced.

2. Experimental

2.1. Balance of Plant

The electrolyser tests were performed with a prototype 12 kW stack from Nel (formerly Proton Onsite). The stack is rated for hydrogen outlet pressures up to 350 bar (differential pressure operation), and consists of 34 cells, each with an electrode area of 90 cm^2. The maximum operating current of the stack is 160 A, with a corresponding nominal stack operating voltage of 75 V (Beginning of life) and a hydrogen production rate of 2 $Nm^3\ h^{-1}$.

The test bench used for the tests was described in detail elsewhere [28]. It is dimensioned for stacks up to 33 kW and 200 bar differential pressure operation, and most of the key hardware components such as the pressure vessels/tanks, coolers/dryers, filters/mix-beds etc. have been designed and built in-house at IFE. Fig. 2 depicts the front panel of the control application (programmed in LabVIEW) showing the full piping and instrumentation diagram (P&ID) of the BoP. The left side of the stack represents the low-pressure H_2O/O_2 subsystem, and the right side of the stack represents the high-pressure H_2 subsystem. The main water pump (*P-02*) sends water through the thermal management system, consisting of two heat exchangers and one heater, before entering the stack. The heat exchangers have a capacity of 2 and 6 kW_{therm}, respectively, and the electrical heater (8 kW_{el}) is installed to heat the system water to the desired temperature during startup, as well as to maintain the operating temperature when necessary. The temperature control system is set up as a cascade structure where three heater/cooler power proportional–integral–derivative (PID) controllers are controlling the temperature measured directly at the respective output water streams. These controllers are tuned for providing fast temperature response to any change of the setpoint and are tied together by an overall outer PID controller. The outer temperature PID controller is set up to slowly make the water temperature settle on targeted setpoint.

In order to pressurize the hydrogen side, a current is applied to the stack, and the H2 subsystem until the backpressure regulator (CV-08 in Fig. 2). When this reaches the setpoint (5–180 bar), the gas is then released as needed to the gas vent to achieve a constant pressure. The anodic pressure is set to 1.2 bara throughout all the tests, irrespective of the cathodic pressure.

A reverse osmosis unit (Merck Millipore) which produces deionized water and feeds it to a makeup water tank is installed in the system. A small pump (*P-03*) automatically replenishes the water consumed in the electrolysis process upon a signal from a level transmitter in the oxygen/water separator and feeds the water into the parallel water purification loop containing an ion exchange resin (*Fi-02*). The parallel purification loop has been installed to maintain an adequate water quality (>2 MΩ) and thereby prevent contamination of the stack. This loop continuously bleeds off water from the main water circulation loop, and the water quality is monitored using a conductivity measurement instrument (Jumo).

On the H_2 side, the water-level of the high-pressure hydrogen/water separator (*Ta-03*) is regulated based on a signal from a point level transmitter, and the drained water is collected in a second tank at ambient pressure. A back pressure regulator (Pressure Control Solutions B·V.) controls the pressure via reference pressure reading, and mass flow is monitored with the aid of variable area flowmeters (Brooks).

2.2. Power conditioning system

In addition to the high-pressure PEMEL test rig, the hydrogen system laboratory at IFE includes a fuel cell test setup with a 13 kW PEM fuel cell stack (Power Cell) and a battery test bench for operating modules with a power up to 80 kW (Corvus Energy). Each of these setups have their own dedicated, custom-built DC/DC-converters (Hot Platinum), which are coupled to the same DC-bus. This makes it possible to operate all the systems simultaneously, to test various electrical hybridization

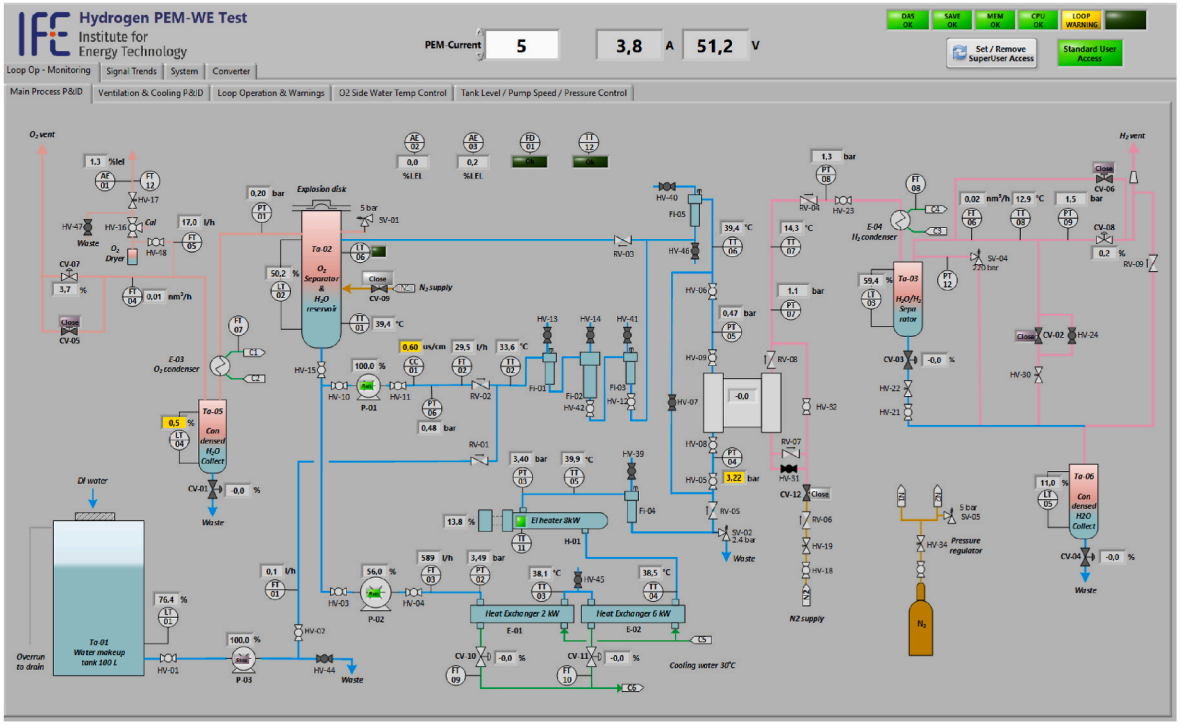

Fig. 2. LabVIEW front panel showing the full P&ID for the system. All installed instrument readings are displayed, and warning or alarm states are indicated by yellow or red background colour, respectively. The various subsystems are also colour coded, where blue is the DI water loop, pink (right) is the H_2 subsystem, green is the cooling system, red (peach) on the left is the O_2 system, and orange is the nitrogen (safety) system. (For interpretation of the references to colour in this figure legend, the reader is referred to the Web version of this article.)

strategies, and to emulate different electric topologies. The heavy-duty li-ion battery can for example be used to test hybrid electric topologies for the water electrolyser system, - a system configuration which may be important for high-pressure electrolysers that cannot operate in load-following mode (due to the risk of gas crossover) in the same manner as more conventional PEMEL-stacks designed for operation at lower pressures (e.g., 15–30 bar).

A cell voltage monitoring (CVM) system is integrated in the electrolysis setup to monitor the state of health of the individual cells and study cell performances and trends across the stack. The individual cell voltages are routinely compared to the average, thereby detecting faulty cells and preventing catastrophic cell failures. The installed CVM system (SMART TESTSOLUTIONS) can provide a sampling rate of up to 1 kHz.

2.3. Safety systems

There are several safety barriers embedded both in the physical setup and in the control system. These include an inline H_2 sensor which continuously monitors the concentration of H_2 in the O_2 stream (AE-01, Pemac), two H_2 sensors in the ceiling of the container for 100 % redundancy (Oldham), a rupture disk on top of the O_2/H_2O separator, a powerful ventilation system (35 ACH) and an N_2 purging system which is automatically triggered in case of, e.g., an H_2 alarm. In the event of a membrane rupture or similar, causing a reverse flow of hydrogen into the anodic subsystems, a check valve is placed directly downstream from the stack to ensure that only a limited volume of hydrogen is able to enter the oxygen subsystem.

The inline H2 sensor (AE-01) is a GE XMTC Panametrics Thermal Conductivity Binary Gas Transmitter gas analyser system, placed downstream from the oxygen/water separator near the O2 gas vent. The system is calibrated regularly using 5% H2 in N2.

2.4. Electrochemical characterisation

Polarization curve analysis was used to characterize the stack performance. Tests were carried out with a water flow rate of 10.2 L min^{-1}, a water inlet pressure of 3.3 bar (absolute pressure), O_2 outlet pressure of 1.2 bar at different temperatures (30, 50 and 80 °C) and H_2 outlet pressures (between 5 and 180 bar). The stack was operated in galvanostatic control. The water conductivity was in the range 0.3–0.5 µScm^{-1} during the tests.

The polarization curve measurements were performed according to the procedure outlined in Ref. [4]. The dwell time and data acquisition time were minimum 30 s each, and the stack current and voltage was averaged over a minimum of 10 data points recorded during the period of data acquisition at each current density step. Ascending and descending polarization curves were recorded.

3. Results

3.1. Electrolyser performance

3.1.1. Polarization curves and voltage efficiency

Fig. 3 depicts the polarization curves recorded between 5 and 180 bar at 30 °C, 50 °C, and 80 °C. To the best of our knowledge, 180 bar is the highest pressure under which polarization data have been recorded and published. The observed trend in stack polarization as a function of temperature and pressure is as expected and as observed in other studies (e.g., Refs. [9,22,29–31]): The stack potential decreases with an increase in temperature or a decrease in pressure.

In Fig. 4, the voltage efficiency in relation to the thermoneutral potential (HHV) is depicted at 160 A (1.86 A cm^{-2}) as a function of temperature and pressure. Here it should be noted that the thermoneutral potential has a small temperature dependency, decreasing from 1.480 V at 30 °C, to 1.477 V at 50 °C, and 1.472 V at 80 °C. As expected, the efficiency increases with temperature, and a maximum of 71% is

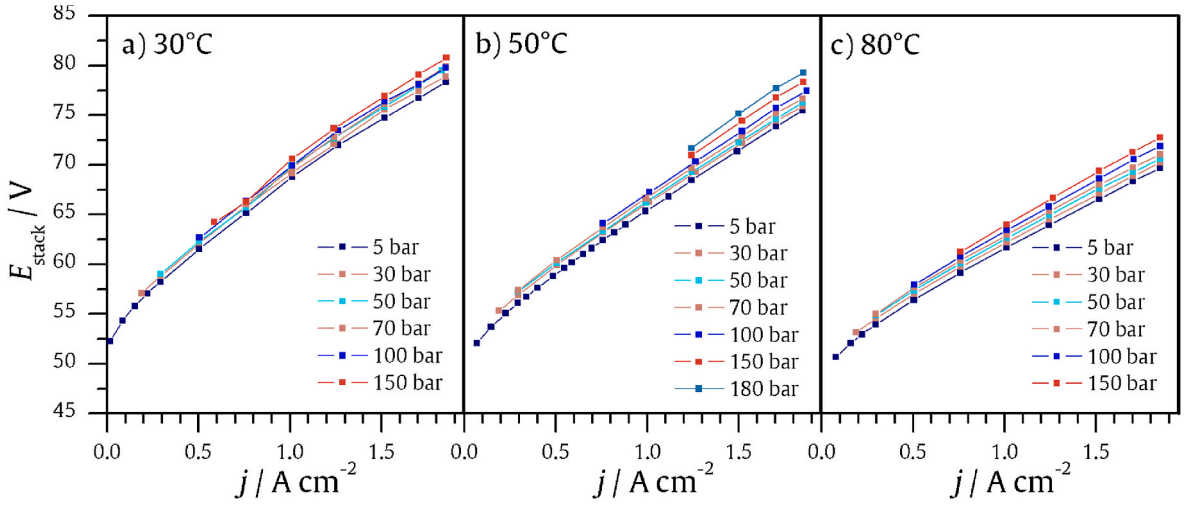

Fig. 3. Polarization curves with total stack potential measured at different temperatures and pressures.

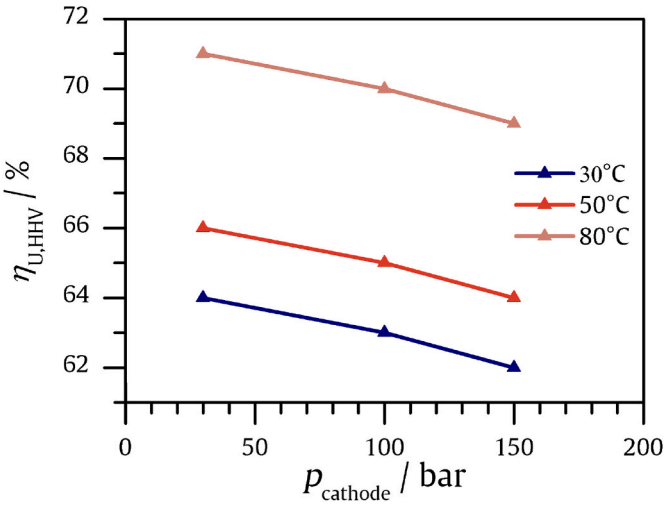

Fig. 4. Voltage efficiency as a function of temperature and pressure.

achieved at 80 °C and 30 bar. At lower temperatures, this drops down to 66% and 64% for 50 °C and 30 °C respectively. The increase in pressure lowers the voltage efficiency, and at 150 bar, the voltage efficiency is 69%, 64%, and 62% for 80 °C, 50 °C, and 30 °C, respectively. The results shown in Fig. 4 underscores the importance of pursuing higher operating temperatures for electrolysers: Whereas the energy penalty associated with a pressure increase from 30 to 150 bar corresponds to 2 kWh kg^{-1}, the energy gain by increasing temperature from 50 °C to 80 °C corresponds to 4.4 kWh kg^{-1}.

With basis in the electrochemical electrolyser model presented in Ref. [1], the polarization curves recorded at 5 bar (presented in Fig. 3) have been fitted by the NLLS method [4,5] to determine the distribution of reversible, ohmic and kinetic losses. The results are presented in Fig. 5. In accordance with the model, the increase in temperature decreases both the reversible, ohmic, and kinetic losses. From the curve fitting, we estimate that the resistivity drops from 0.33 Ω cm^2 at 30 °C, through 0.31 Ω cm^2 at 50 °C, to 0.23 Ω cm^2 at 80 °C. The anodic exchange current density, which was the fitted kinetic parameter, goes from 3.1•10^{-13} A cm^{-2} at 30 °C, through 2.1•10^{-11} A cm^{-2} at 50 °C, to 2.3•10^{-10} A cm^{-2} at 80 °C. The reversible (thermodynamic) potential decreases only slightly, by 2.6% from 30 °C to 80 °C. These factors together lead to the increase in voltage efficiency, represented in Fig. 4, of 7 percentage points when increasing temperature from 30 to 80 °C.

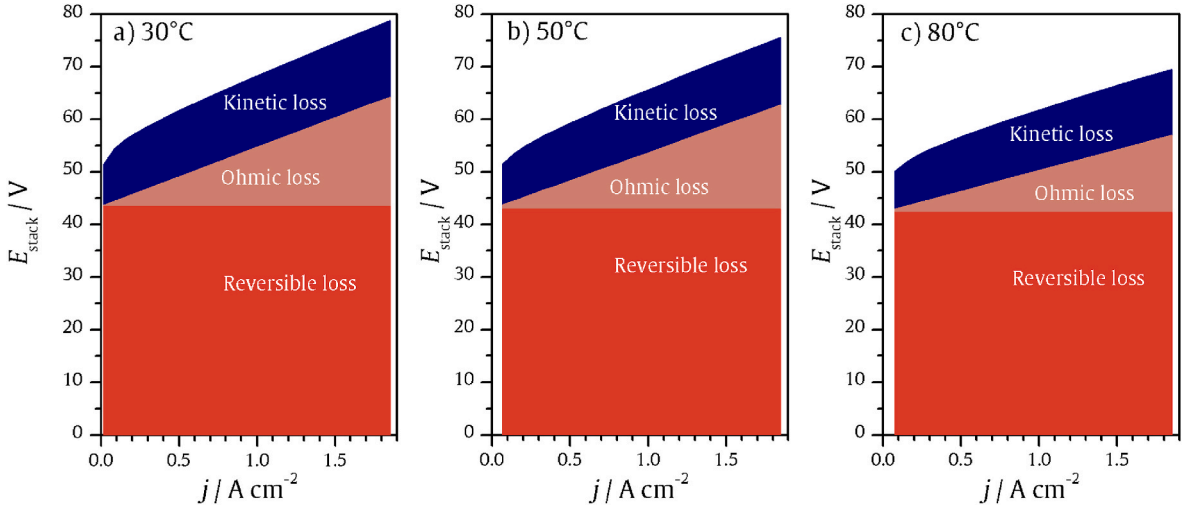

Fig. 5. Polarization curves at 5 bar with model fit for reversible, ohmic, and kinetic losses at a) 30 °C, b) 50 °C, and c) 80 °C.

3.1.2. Faradaic efficiency

The faradaic efficiency is an important consideration as it influences the overall efficiency of the system. Higher differential pressures will give reverse flow of hydrogen across the membrane (crossover), and subsequently reduce the faradaic efficiency (hydrogen crossover is primarily governed by concentration-driven and pressure-driven diffusion [9]). From the measured hydrogen production rate and the relation to the applied current, the faradaic efficiency can be estimated, but it requires careful experimental setup and design to achieve a high accuracy [12–14]. Fig. 6 depicts results from the measurements performed at the setup at IFE, using variable area flowmeters, after the necessary corrections for operating pressure have been performed. Here, the measured average flow at 50 °C at two current densities are shown as a function of cathodic pressure. The measured data are compared to the theoretical maximum (i.e., assuming no crossover) and the modelled flow according to the gas crossover model first presented in Ref. [9]. Although the experimental data scatter significantly, the measured flow rate can be seen to drop with increasing H_2 pressure and decreasing current density, just as expected. The faradaic efficiency can be calculated as the ratio between the theoretical maximum and the actual flow: At 1.50 A cm^2, the measured faradaic efficiency drops from 99% to 90% when moving from 30 to 70 bar, whereas at 1.86 A cm^{-2}, the measured faradaic efficiency vary from 96% at 5 bar to 88% at 50 bar. Due to the use of a variable area flowmeter, the flow measurements have large uncertainty, and it was therefore decided to use the modelled results (solid lines in Fig. 6) in the analysis below.

3.1.3. Compresssion losses

In Fig. 7 the compression losses at different compression ratios are shown. Fig. 7a shows the voltage compression loss at 50 °C and 80 °C, extracted from Fig. 4, and Fig. 7b shows the sum of the voltage compression loss and the faradaic compression loss 50 °C. The faradaic loss was calculated from the ratio between the stippled line and solid line in Fig. 6.

In Fig. 7a the measured voltage loss is compared to the theoretical voltage loss as defined by the Nernst potential. Interestingly, compression from 5 to 30 bar yields a smaller compression loss than expected and suggests that the electrochemical performance effectively improves (when the thermodynamic loss has been corrected for). A similar observation was made in Ref. [32], and in this case it was speculated whether this was caused by improved electrode kinetics at higher operating pressures. Above 30 bar, however, the compression losses are larger than the thermodynamic model suggest, and this deviation increases with increasing pressure. This could, for example, be due to increased contact resistance at the cathode, but would have to be investigated in more detail using, e.g., electrochemical impedance spectroscopy. From these observations it can be concluded that even though the most commonly adopted electrochemical models for PEM electrolysis assumes that only the Nernst potential exhibits a pressure dependency, it may be necessary to revisit the models and consider the effect of pressure on the kinetic and ohmic losses as well. This was indeed done in a recent paper [26] in which the pressure influence on the activation overpotential term was assessed.

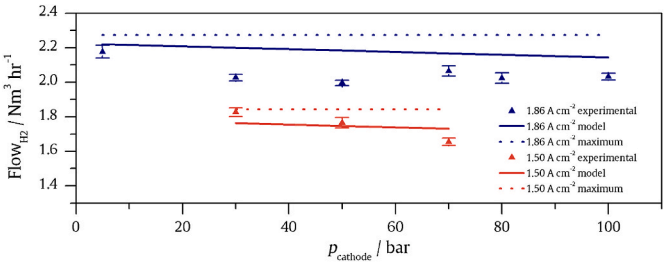

Fig. 6. Measured flow at different current densities as a function of system pressure at a temperature of 50 °C. Comparison with modelled and theoretical maximum values.

In Fig. 7b the total electrochemical compression loss (sum of voltage loss and faradaic loss) for different compression steps at 50 °C are summed up and compared to the alternative mechanical compression energy (assuming adiabatic compression) [1]. The data shows that for the lower compression range from 5 to 30 bar, electrochemical compression has a large advantage compared to mechanical compression. The additional energy use compressing the gas from 30 to 50 bar is similar for mechanical and electrochemical compression, whereas going to 100 or 150 bar using only the electrolyser is energetically unfavorable.

It is well known that the first compression stage (to about 30 bar) should be performed internally in the electrolyser for higher efficiency because the large compression ratio and the corresponding high CAPEX of the compressor makes the compression stage inefficient [33]. Interestingly, our work shows that it is even more advantageous for the electrolyser to handle the first compression stage than thermodynamics would suggest, taking into account the relative performance gain depicted in Fig. 7a. For compression to higher pressures than 30 bar, there is a tradeoff between the increase in energy use and the savings in CAPEX.

In our previous work [1] we showed that for all the considered pressure states (80, 200, 350 and 700 bar), the energy penalty associated with pure electrochemical compression was higher than for a combination of electrochemical and mechanical compression. It was therefore concluded that the business case for high-pressure PEM electrolysis heavily relies on the cost of energy, which needs to be sufficiently low. From the experimental work here, showing that the increase in overvoltage with pressure is considerably larger than expected, it can be argued that even lower electricity prices than those depicted in Fig. 7 in Ref. [1] are needed to achieve a viable business case for high-pressure electrolysis.

3.1.4. Cell performance

Individual cell voltage measurements are useful in identifying whether any of the cells perform significantly worse and could aid in the preventative maintenance of the stack. In Fig. 8 the individual cells voltages during stack testing at 30 bar and 50 °C are presented. Except for the first cell in the stack (on top of the stack), all cells fell within a narrow range of potentials having a variation of less than ±1.54%. Such a value is indicative that the cells perform as prescribed and that there is no significant degradation difference on the cells. The first cell is the outlier and show significantly higher cell voltage, about 3–4% higher than the cell average of the other cells. This indicates that it either experiences different temperatures to the other cells (it is the end cell), or that some degradation has taken place. The nature and source of this deviation was however not investigated further.

3.1.5. Water management

The water transport through the membrane from the anode to the cathode is an equilibrium established between three processes: electroosmotic drag transport, diffusion transport, and hydraulic pressure transport [17]. Increasing the cathodic operating pressure will therefore contribute to lowering the humidity-level of the produced H_2 gas and will thus reduce or eliminate the need for downstream gas drying (depending on end-use application) [17,34]. Conflicting results have however been reported for the effect of pressure and current density on the net water drag coefficient in PEM water electrolysis [17,22], and it is therefore a need to further understand the relation between the processes governing water drag. Since the total water crossover is the sum of the water discharged from the hydrogen/water separator (*Ta-03* in Fig. 2) and the humidity in the vented hydrogen (100 % RH), the water crossover rate can be quantified by integrating the water release from the separator during steady state conditions. In Fig. 9, the water crossover has been quantified at varying pressure and two different current

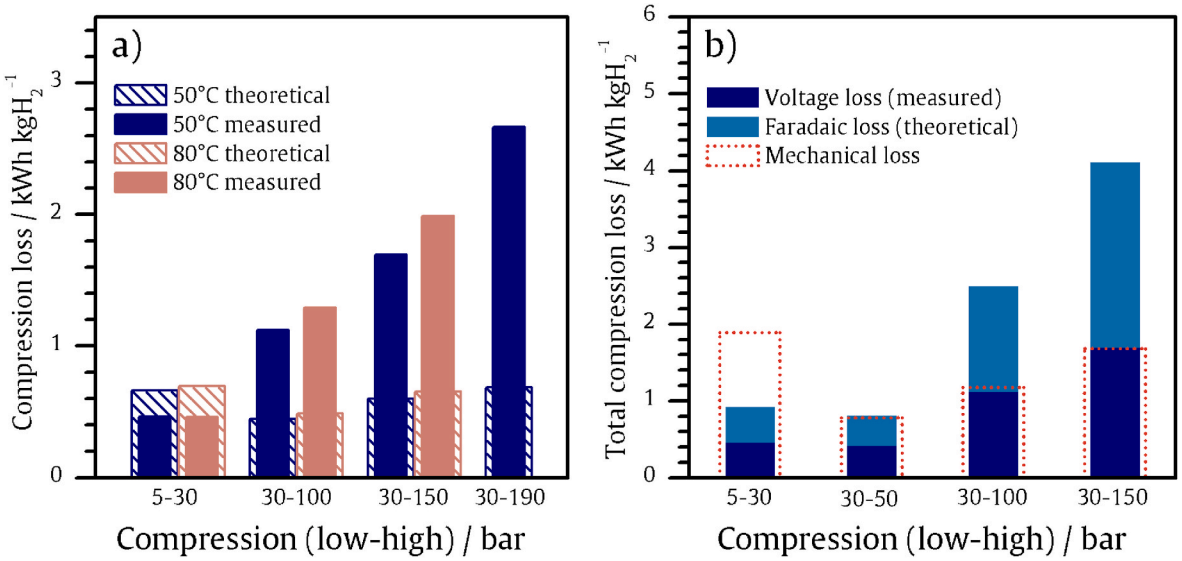

Fig. 7. Compression loss, a) Theoretical vs measured voltage loss at various compression ratios and temperatures (50 °C and 80 °C), b) Estimated *total* electrochemical compression loss from measured voltage loss and theoretical Faradaic loss at 50 °C, comparison with modelled data of mechanical compression losses in Ref. [1].

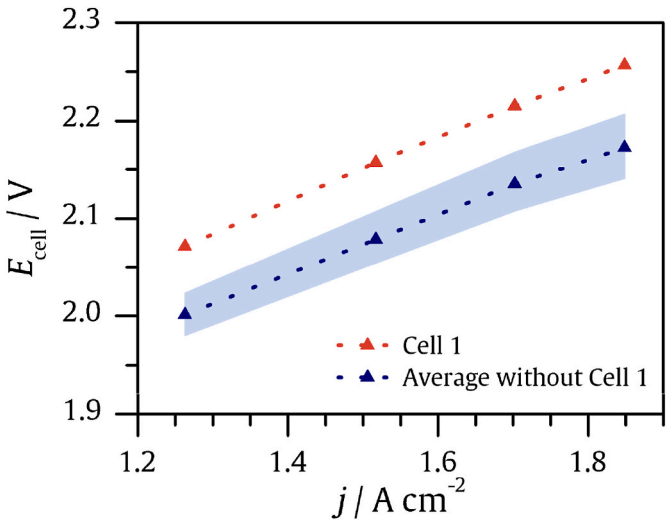

Fig. 8. Cell voltage data showing normal deviation of the cells and the outlier cell 1.

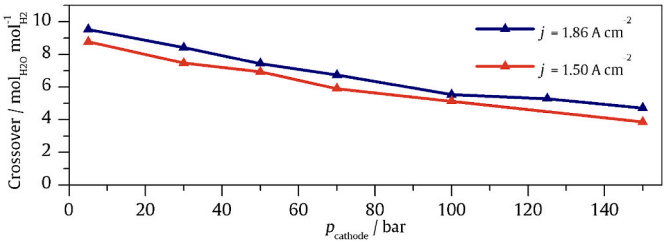

Fig. 9. Water crossover as a function of pressure and current density. All results at a temperature of 50 °C.

densities. As expected from the water transport mechanisms, the water drag is reduced when increasing the cathodic pressure and increased when increasing the current density. This is in accordance with the results of Medina et al. [17], but in conflict with the findings of Suermann et al. [22] who could only observe a temperature-dependency of the water drag. The drag coefficient found in this work is almost twice of what was measured in the work by Medina et al. [17], but it should be noted that they measured at a lower current density of 1 A cm^{-1}. The results in Fig. 9 underscores the added advantage of increasing the differential pressure in that the humidity level of the product gas is reduced. As the water transport is significant, i.e., up to 10 times the production rate of hydrogen, this effect is significant in terms system size and optimization because the cathodic water needs to be released or recycled.

3.2. System performance

3.2.1. Thermal management

As the experimental BoP used in this work has advanced temperature control and more sensors than a commercially available system, it is possible to analyse the performance of the thermal management system. This is useful to be able to optimize the design and control of such systems, and to better understand the overall energy use. In Fig. 10, the stack power, heating power, cooling power (left y-axis), along with the outlet and inlet water temperature of the stack (right y-axis) are plotted as a function of time meanwhile stepping down the stack current (stack power) at three different operating temperatures. Notably, in our setup, the stack temperature corresponds to the water outlet temperature and is controlled by the stack inlet temperature through the thermal management system. In Fig. 10 the outlet water temperature and stack voltage is shown as a function of current density for the same three temperatures.

At low temperatures (30 °C in Fig. 9a), the system struggles to maintain a constant temperature, and the throttle valves for the heat exchangers are fully open. At this point, more than 70% of the stack power is used to cool the system. The cooling system has a nominal cooling power of 8 kW, however, since the temperature difference between the cooling water and the water circulation system (10–20 K at 30 °C) is small, the real cooling power is smaller than 8 kW. This demonstrates that the thermal management system does not perform well under these operating conditions, something which is further evidenced by Fig. 11a. Here it is shown that the outlet water temperature increases with increasing current density, and reaches 35 °C at the peak current. Under these conditions it should also be noted that there is a significant temperature difference over the stack (about 4 °C), suggesting that the individual cells experience different degrees of degradation

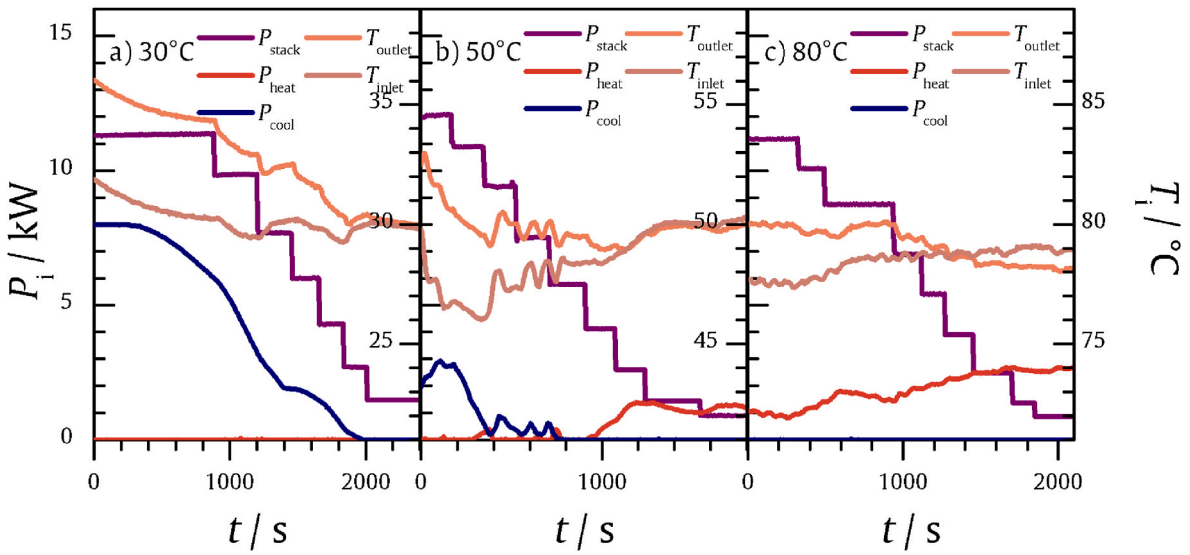

Fig. 10. Power curves, outlet temperature, and inlet temperature at 30 bar hydrogen pressure for the temperatures a) 30 °C, b) 50 °C, and c) 80 °C.

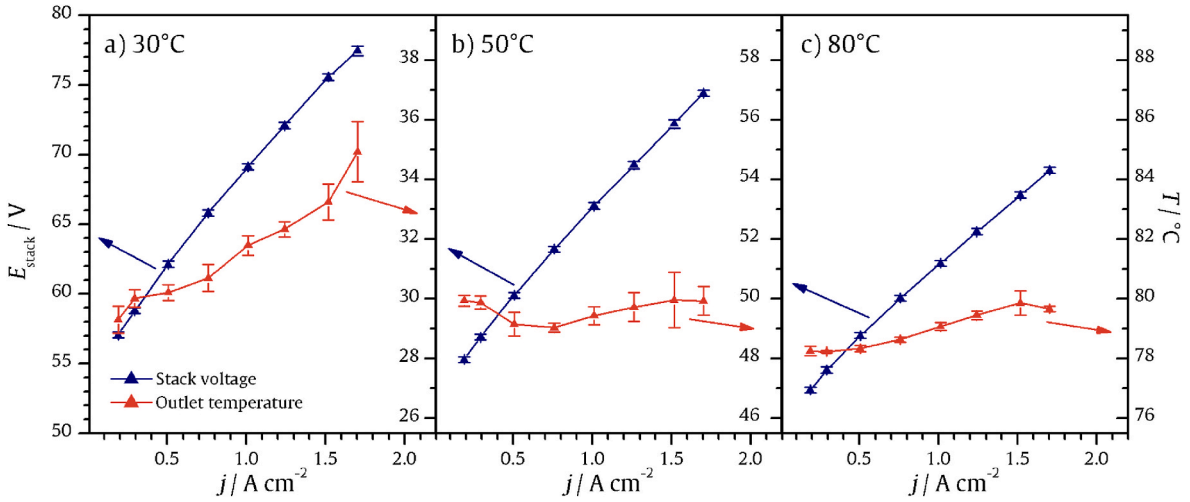

Fig. 11. Stack voltage and outlet temperature as a function of current density at a) 30C, b) 50 °C, and c) 80 °C. The hydrogen pressure was 30 bar. All stack voltage results are on the same scale.

(typically higher at colder cells). When the stack power is decreased, a system-specific optimum at 2–4 kW system power where neither heating nor cooling is needed is revealed.

For the case at 50 °C, Fig. 10b, much less cooling is needed to keep the system stable in temperature, and as the stack power is decreased, even external heating is needed. Here, the heater and coolers are sufficient to keep the water outlet temperature close to the nominal temperature of 50 °C, as shown in Fig. 11b. The operating optimum where neither cooling nor heating is needed is in this case found at about 4–6 kW. This is considerably higher than at 30 °C, but still far from the maximum power of the stack (12 kW in our case). At 50 °C it can also be observed in Fig. 9b that the temperature ripples (±0.8 K) are particularly prominent in a certain current density region. These arise because the regulator alternates between cooling and heating, and indicates that the PID controllers of the thermal management system could be further finetuned for these operating conditions.

At the highest temperature, 80 °C in Fig. 10c, no cooling is needed, and heating is necessary during the whole range of stack power. This condition may change if the stack is larger and has higher heat production and thermal capacity. The temperature difference over the stack is also smaller, maximum 2.5 °C, which means that the system operates more isothermally ensuring more stable conditions. At the highest stack power, the optimum condition occurs where about 10% of the stack power is necessary as heating. While system specific, one can envision that each stack power has its optimum temperature where minimum heating and cooling power is applied. At the highest current density, 1.86 A cm^{-2}, this optimum is around 70 °C for the stack used here. It is thus possible to identify such system-level thermoneutral optima in order to operate the system in the most efficient way.

3.2.2. *Hydrogen safety*

Hydrogen safety must be carefully handled when operating PEM water electrolysers at high differential pressures, especially when intermittent power sources are considered as the supply of energy. The reverse flow of hydrogen through the membrane to the oxygen side which represents a particular safety challenge [8], and usually, a recombination catalyst is incorporated in the membrane electrode assembly (MEA) to ensure that the hydrogen content in the oxygen is below the lower flammability limit (4% H_2 in O_2) [15]. The measured concentration of hydrogen in the produced oxygen is shown in Fig. 12 as a function of current density and system pressure. In this case, the current density is stepped down from 1.86 A cm^{-2} to 0.50 A cm^{-2} while the

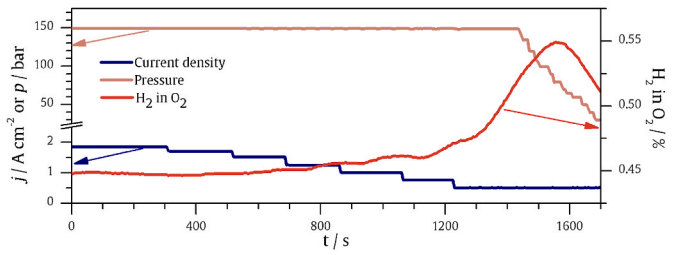

Fig. 12. Trend of H2 in O2 when the current is reduced at 150 bar differential pressure. Temperature is 30 °C.

hydrogen pressure at the cathode is kept constant at 150 bar. The hydrogen concentration is initially at about 0.45 % (ca 11% of LFL) and increases gradually as the current is reduced. At each current density, the hydrogen concentration in the oxygen reaches a stable value which represents an equilibrium between the crossover rate, reaction rate at the recombination catalyst, and the diffusion of reactants toward the recombination catalyst. When reducing the current density to 0.50 A cm^{-2}, the production rate is too low to hinder the hydrogen crossover, and the H_2 concentration increases rapidly making it necessary to reduce the system pressure due to safety. This shows that tests like these can serve to map the safe operating window of PEM electrolysers at different working pressures, an exercise which is very important if intermittent operation is considered. The lower current density limit of 0.50 A cm^{-2} encountered in this example corresponds to a turndown of 25%. A larger turndown range will be available at lower operating pressures and at ambient pressure, full turndown should be possible.

4. Conclusions

The removal of an external hydrogen compressor by increasing the operating pressure of PEM electrolysers is a promising approach to reduce the cost of green hydrogen, in particular where the delivery pressure does not exceed 200 bar. In this work, the performance of a differential-pressure PEMEL system has been characterized as a function of current density between 5 and 180 bar at 30 °C, 50 °C and 80 °C. The following conclusions can be made:

- The voltage efficiency at 50 °C decreases from 66 % at 30 bar to 64 % at 150 bar, corresponding to a compression loss of ca 2 kWh kg^{-1}. In contrast, the energy saving associated with a temperature increase from 50 to 80 °C was found to be 4.4 kWh kg^{-1}.
- The water drag from the anode to the cathode was more than halved (reduced from 9 mol_{H20} mol_{H2}^{-1} to 4 mol_{H20} mol_{H2}^{-1}) when increasing the pressure from 5 to 150 bar at 1.5 A cm^{-2}.
- Measurement of hydrogen-content in oxygen during operation can serve to map the safe operating window of PEM electrolysers at different working pressures. Example given, it was shown that at 150 bar differential pressure, the maximum turndown range is 25%, corresponding to a current density of 0.5 A cm^{-2}.
- It is observed that compression effectively improves the electrochemical performance in the lower pressure range (from 5 to 30 bar), whereas further pressurization, e.g., up to 100 and 150 bar, reduces the performance significantly. The findings reveals that the standard electrochemical models do not account for the impact of pressure on the kinetic and/or ohmic losses.
- Since the measured electrochemical compression loss is larger than previously modelled, even lower energy costs than previously anticipated in modeling work are needed to make an economically viable system.

From the observations reported in this work, several questions remain regarding the optimization of high-pressure PEM water electrolysis systems and how this will affect the overall costs in comparison to state-of-the-art systems. The business case relies on tradeoffs such as the potential for system cost savings by removing the mechanical compressors and being able to build more compact, silent and vibration free systems, vs. the increased CAPEX of the electrolyser (more expensive components and complex designs). From an efficiency and safety point-of-view, the performance will rely heavily on the membrane thickness and embedded reinforcement and recombiner technology, components expected to be further optimized in commercial products. Finally, longer test campaigns than those carried out in this work will be necessary to quantify degradation driven by the pressure gradient. While high-pressure electrolysis has shown some promise, especially in the 80–200 bar range [1], further validation is necessary before it can justify deployment.

CRediT authorship contribution statement

Ragnhild Hancke: Writing – review & editing, Writing – original draft, Formal analysis, Data curation. **Piotr Bujlo:** Writing – review & editing, Investigation, Formal analysis, Data curation. **Thomas Holm:** Writing – original draft, Investigation, Formal analysis, Data curation. **Øystein Ulleberg:** Writing – review & editing, Funding acquisition, Conceptualization.

Declaration of competing interest

The authors declare that they have no known competing financial interests or personal relationships that could have appeared to influence the work reported in this paper.

Data availability

Data will be made available on request.

Acknowledgements

This work was supported by the Norwegian Research Council through the research infrastructure "*Norwegian Fuel Cell and Hydrogen Centre*" (grant number 245678) and "*FME MoZEES*", a Norwegian Centre for Environment-friendly Energy Research (grant number 257653).

References

[1] R. Hancke, T. Holm, Ø. Ulleberg, The case for high-pressure PEM water electrolysis, Energy Convers. Manag. (2022) 261.
[2] K.E. Ayers, et al., Research advances towards low cost, high efficiency PEM electrolysis, ECS Trans. 33 (1) (2010) 3–15.
[3] E. Haryu, K. Nakazawa, K. Taruya, Mechanical Structure and Performance Evaluation of High Differential Pressure Water Electrolysis Cell, vol. 23, Honda R&D Technical Review, 2011.
[4] S.A. Grigoriev, et al., High-pressure PEM water electrolysis and corresponding safety issues, Int. J. Hydrogen Energy 36 (3) (2011) 2721–2728.
[5] T. Holm, et al., Hydrogen costs from water electrolysis at high temperature and pressure, Energy Convers. Manag. (2021) 237.
[6] V.I. Bolobov, Mechanism of self-ignition of titanium alloys in oxygen, Combust. Explos. Shock Waves 38 (6) (2002) 639–645.
[7] M.N.I. Salehmin, et al., High-pressure PEM water electrolyser: a review on challenges and mitigation strategies towards green and low-cost hydrogen production, Energy Convers. Manag. (2022) 268.
[8] S.A. Grigoriev, et al., Hydrogen safety aspects related to high-pressure polymer electrolyte membrane water electrolysis, Int. J. Hydrogen Energy 34 (14) (2009) 5986–5991.
[9] M. Schalenbach, et al., Pressurized PEM water electrolysis: efficiency and gas crossover, Int. J. Hydrogen Energy 38 (35) (2013) 14921–14933.
[10] E. Afshari, et al., Performance assessment of gas crossover phenomenon and water transport mechanism in high pressure PEM electrolyzer, Int. J. Hydrogen Energy 46 (19) (2021) 11029–11040.
[11] J. Dang, et al., Experiments and microsimulation of high-pressure single-cell PEM electrolyzer, Appl. Energy (2022) 321.
[12] J. Dang, et al., Hydrogen crossover measurement and durability assessment of high-pressure proton exchange membrane electrolyzer, J. Power Sources (2023) 563.

[13] M. Bernt, et al., Analysis of gas permeation phenomena in a PEM water electrolyzer operated at high pressure and high current density, J. Electrochem. Soc. 167 (12) (2020).
[14] P. Trinke, et al., Hydrogen permeation in PEM electrolyzer cells operated at asymmetric pressure conditions, J. Electrochem. Soc. 163 (11) (2016) F3164–F3170.
[15] P. Millet, et al., Scientific and engineering issues related to PEM technology: water electrolysers, fuel cells and unitized regenerative systems, Int. J. Hydrogen Energy 36 (6) (2011) 4156–4163.
[16] Q. Feng, et al., A review of proton exchange membrane water electrolysis on degradation mechanisms and mitigation strategies, J. Power Sources 366 (2017) 33–55.
[17] P. Medina, M. Santarelli, Analysis of water transport in a high pressure PEM electrolyzer, Int. J. Hydrogen Energy 35 (11) (2010) 5173–5186.
[18] F. Marangio, M. Santarelli, M. Cali, Theoretical Model and Experimental Analysis of a High Pressure PEM Water Electrolyser for Hydrogen Production, 2009.
[19] M. Santarelli, P. Medina, M. Calì, Fitting regression model and experimental validation for a high-pressure PEM electrolyzer, Int. J. Hydrogen Energy 34 (6) (2009) 2519–2530.
[20] M. Sartory, et al., Theoretical and experimental analysis of an asymmetric high pressure PEM water electrolyser up to 155 bar, Int. J. Hydrogen Energy 42 (52) (2017) 30493–30508.
[21] J. Sieverman, Validation of an advanced high-pressure PEM electrolyzer and composite hydrogen storage, Proton Energy System (2020).
[22] M. Suermann, et al., High pressure polymer electrolyte water electrolysis: test bench development and electrochemical analysis, Int. J. Hydrogen Energy 42 (17) (2017) 12076–12086.
[23] A. Müller-Dollinger, et al., Balanced high pressure PEM electrolysis in batch process up to 110 bar: test bench development and electrochemical analysis, Int. J. Hydrogen Energy (2023).
[24] D. Saebea, et al., Analysis of unbalanced pressure PEM electrolyzer for high pressure hydrogen production, Chemical Engineering Transactions 57 (2017) 1615–1620.
[25] F. Scheepers, et al., Improving the efficiency of PEM electrolyzers through membrane-specific pressure optimization, Energies 13 (3) (2020).
[26] G. Correa, et al., Pressurized PEM water electrolysis: dynamic modelling focusing on the cathode side, Int. J. Hydrogen Energy 47 (7) (2022) 4315–4327.
[27] H. Kim, M. Park, K.S. Lee, One-dimensional dynamic modeling of a high-pressure water electrolysis system for hydrogen production, Int. J. Hydrogen Energy 38 (6) (2013) 2596–2609.
[28] R. Hancke, et al., High differential pressure PEMWE system laboratory, in: EFCF 2019 Low-Temperature Fuel Cells, Electrolysers & H2 Processing, Lucerne, 2019.
[29] M. Carmo, et al., A comprehensive review on PEM water electrolysis, Int. J. Hydrogen Energy 38 (12) (2013) 4901–4934.
[30] S.A. Grigoriev, et al., Current status, research trends, and challenges in water electrolysis science and technology, Int. J. Hydrogen Energy 45 (49) (2020) 26036–26058.
[31] M. Schalenbach, et al., Acidic or Alkaline? Towards a new perspective on the efficiency of water electrolysis, J. Electrochem. Soc. 163 (11) (2016) F3197–F3208.
[32] M. Bernt, H.A. Gasteiger, Influence of ionomer content in IrO2/TiO2 electrodes on PEM water electrolyzer performance, J. Electrochem. Soc. 163 (11) (2016) F3179–F3189.
[33] U. Babic, et al., Critical review-identifying critical gaps for polymer electrolyte water electrolysis development, J. Electrochem. Soc. 164 (4) (2017) F387–F399.
[34] M.N.I. Salehmin, et al., High-pressure PEM water electrolyser: a review on challenges and mitigation strategies towards green and low-cost hydrogen production, Energy Convers. Manag. 268 (2022) 115985.